The inversion of data from complex 3-D resistivity and I.P. surveys

M.H.Loke (Geotomo Software, Malaysia)

K. Frankcombe (ExploreGeo, Australia)

D. F. Rucker (Hydrogeophysics Inc, USA)

Email : drmhloke@yahoo.com

Outline

1. From 2-D to 3-D to 4-D geoelectrical surveys
2. Least-squares inversion method
3. Irregular topography
4. Large I.P. effects
5. Non-rectilinear survey layouts
6. Case histories
7. Conclusions

From 2-D to 3-D to 4-D geoelectrical surveys

2-D electrical imaging surveys are now widely used. However, in very complex environments, a 3-D model is required for sufficient accuracy. Some surveys map temporal changes from repeated 3-D surveys (4-D).

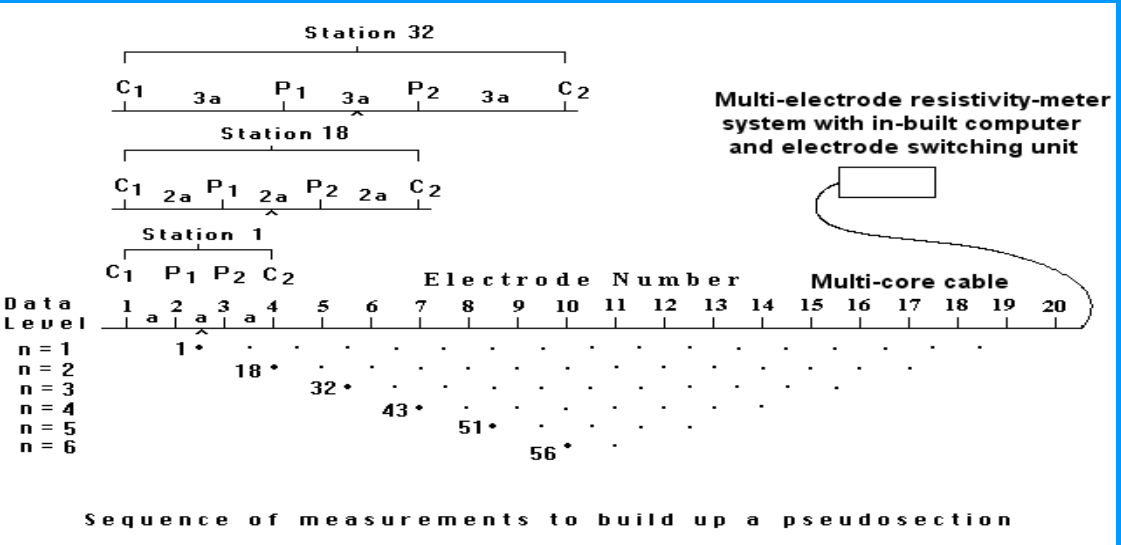

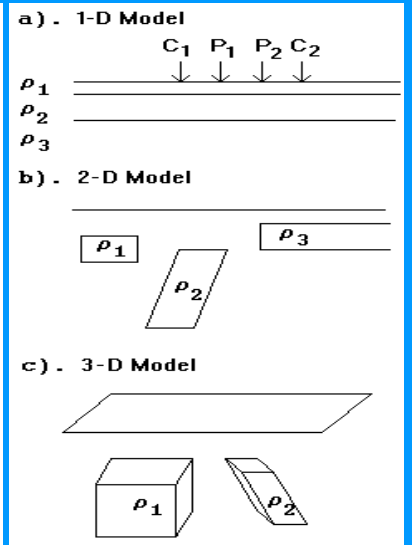

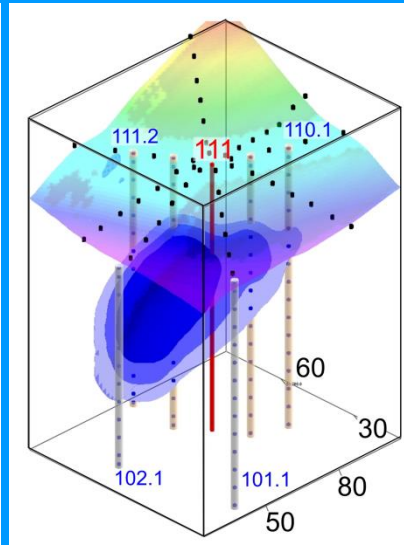

Least-squares inversion method

3-D surveys can have about 100,000 data points, and the interpretation model 100,000 cells. The smoothness-constrained least-squares method is commonly used for such large scale problems.

$$\left(\mathbf{J}^{\mathrm{T}}\mathbf{J}+\lambda\mathbf{F}\right)\Delta\mathbf{q}_{\mathbf{k}}=\mathbf{J}^{\mathrm{T}}\mathbf{g}-\lambda\mathbf{F}\mathbf{q}_{\mathbf{k}-1}$$

F contains the roughness filters and other constraints that stabilizes the inversion, λ is a damping factor, $\Delta\mathbf{q}$ is the change in model resistivity values, and **g** is the data misfit. **J** is the Jacobian matrix of partial derivatives.

The data is the apparent resistivity and I.P. values.

3-D model used

The 3-D model consists of a large number of cells. The size and positions of the cells are fixed, but the resistivity and I.P. chargeability are allowed to vary. Diagonal roughness filters are used to avoid directional bias in the model.

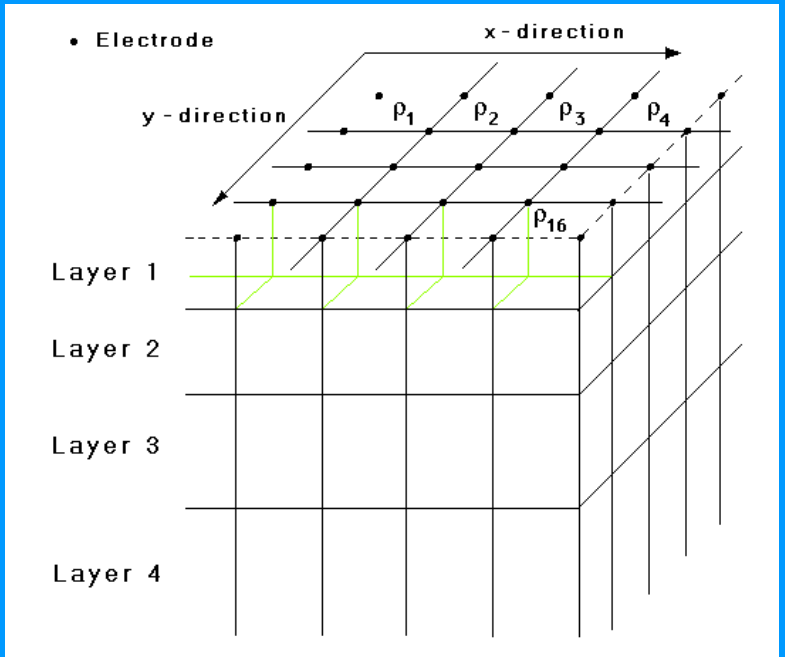

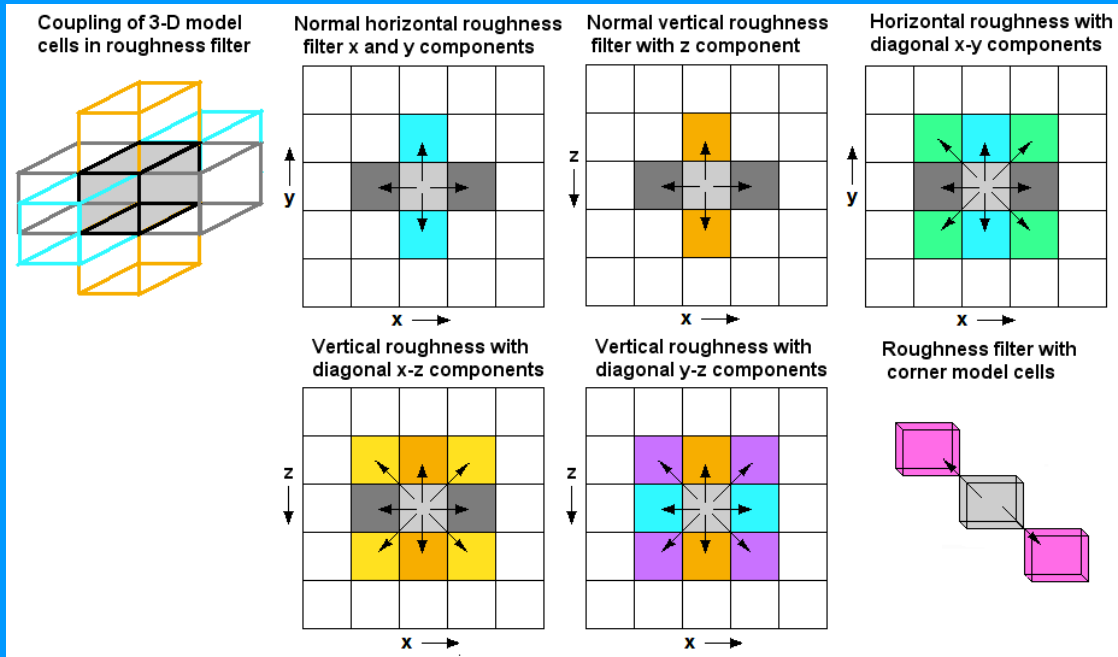

Modeling challenges from modern mineral surveys

The quest for base and precious metals has led to surveys over complex deposits and in extreme terrains using non-conventional arrays. Challenges to realistic inversion models include :-

1. **Extreme topography**
2. **Calculating I.P. effects for non-conventional arrays**
3. **Non-rectilinear, arbitrary survey grids**

Challenging topography

Mineral deposits have an unfortunate tendency to occur in areas with significant topography. To interpret the data from such surveys, the modeling technique used must accurately take into account the topography. The two main forward modeling techniques are the finite-difference and finite-element methods.

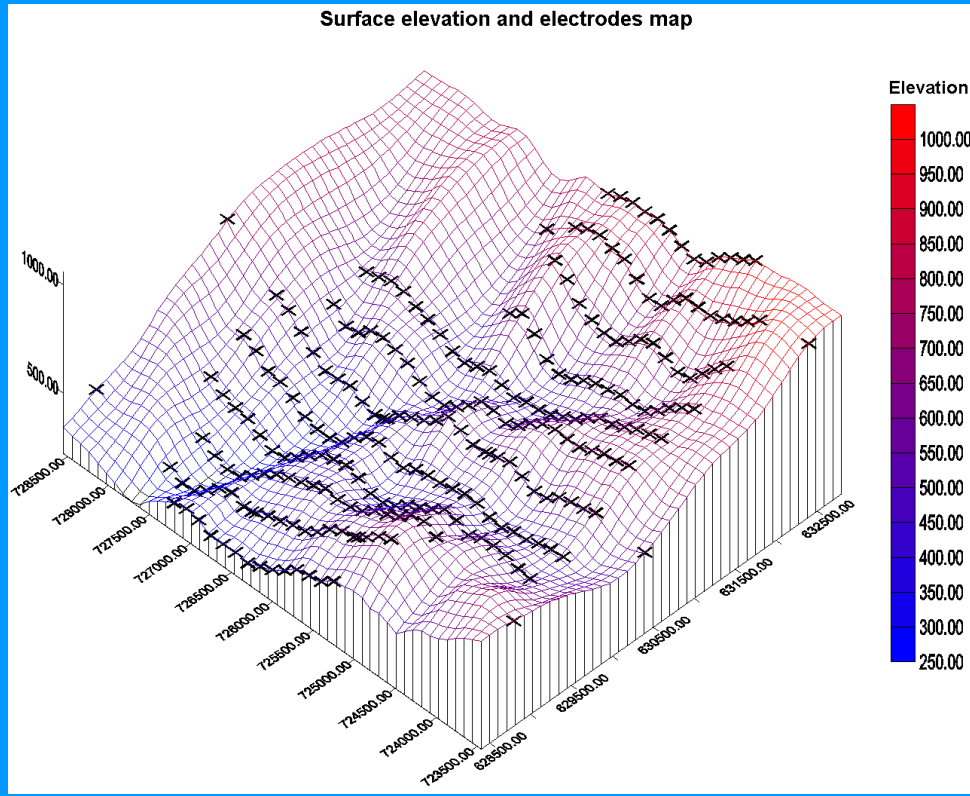

Finite-difference and finite-element methods

The finite-difference method normally uses a rectangular mesh. The surface topography is modeled by small rectangular steps with the mesh cells above the ground assigned a very high resistivity value.

In finite-element method, the position of the nodes can be adjusted to match the topography. Thus the topography is directly incorporated into the inversion model.

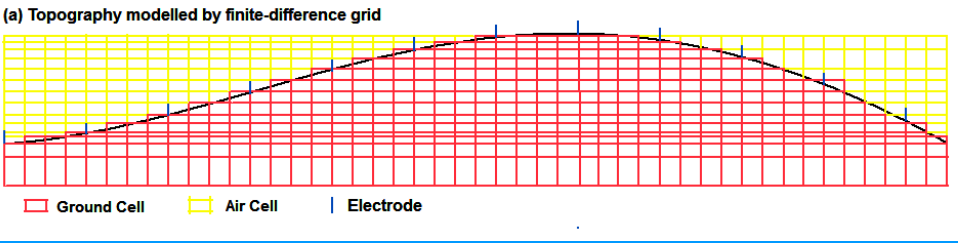

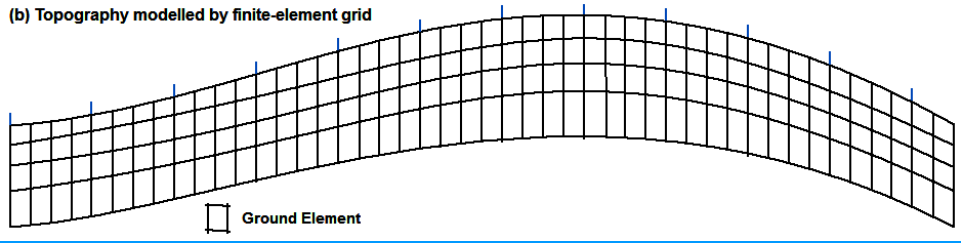

I.P. modeling methods

The two approaches in modeling I.P. data are the perturbation and complex resistivity methods.

The perturbation method considers the I.P. model as a 'small' change from a base resistivity model with conductivity σ_{DC} that is measured by a resistivity survey. The chargeability *m* is to decrease the effective conductivity to $\sigma_{IP} = (1 - m)\sigma_{DC}$. The apparent IP is then calculated by two forward models using the original and perturbed conductivities, such as

$$m_a = [\, \phi(\sigma_{IP}) - \phi(\sigma_{DC}) \,] / \phi(\sigma_{DC})$$

where ϕ is the potential calculated by the finite-element method. There are two main problems with this approach.

Problems with perturbation method

(1). Its is based on the assumption the chargeability is ‘small’.

(2). The method used to calculated the apparent I.P.

$$m_a = [\, \phi(\sigma_{IP}) - \phi(\sigma_{DC}) \,] / \phi(\sigma_{DC})$$

is sensitive to errors in the forward modeling method, particularly when $\phi(\sigma_{DC})$ is small. In some situations it might even be negative, particularly with the new ‘offset’ type of arrays. In such cases, the calculated m_a values are not reliable.

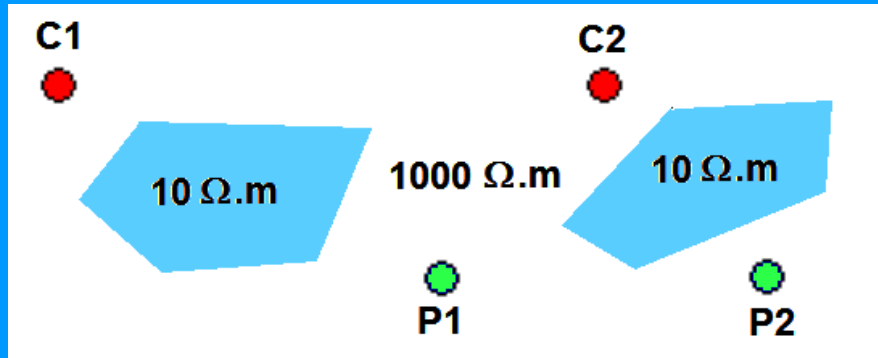

IP modeling – the complex resistivity method

The conductivity is treated as a complex quantity that is given by

$$\sigma = \sigma_{DC} - i\, m.\sigma_{DC}$$

The DC conductivity σ_{DC} forms real part, while $m.\sigma_{DC}$ forms the imaginary part. A complex potential is then calculated.

$$\phi = \phi_r + i\, \phi_i$$

The apparent resistivity value is calculated by using the amplitude of the complex potential, $\phi_A = (\phi_r^2 + \phi_i^2)^{0.5}$. The apparent chargeability is calculated using the ratio of the imaginary and real components, $m_a = \phi_i / \phi_r$. The accuracy of m_a does not depend on the D.C. potential accuracy.

Non-rectilinear survey grids

While modern 3-D surveys attempt to use an arrangement with parallel survey lines, it might be necessary to deviate the lines due to topographical obstructions. In some areas, old data from 2-D surveys lines are reinterpreted using modern software. The survey lines frequently have different directions.

For such data, a flexible model discretisation is needed. The model grid is independent of the electrodes layout.

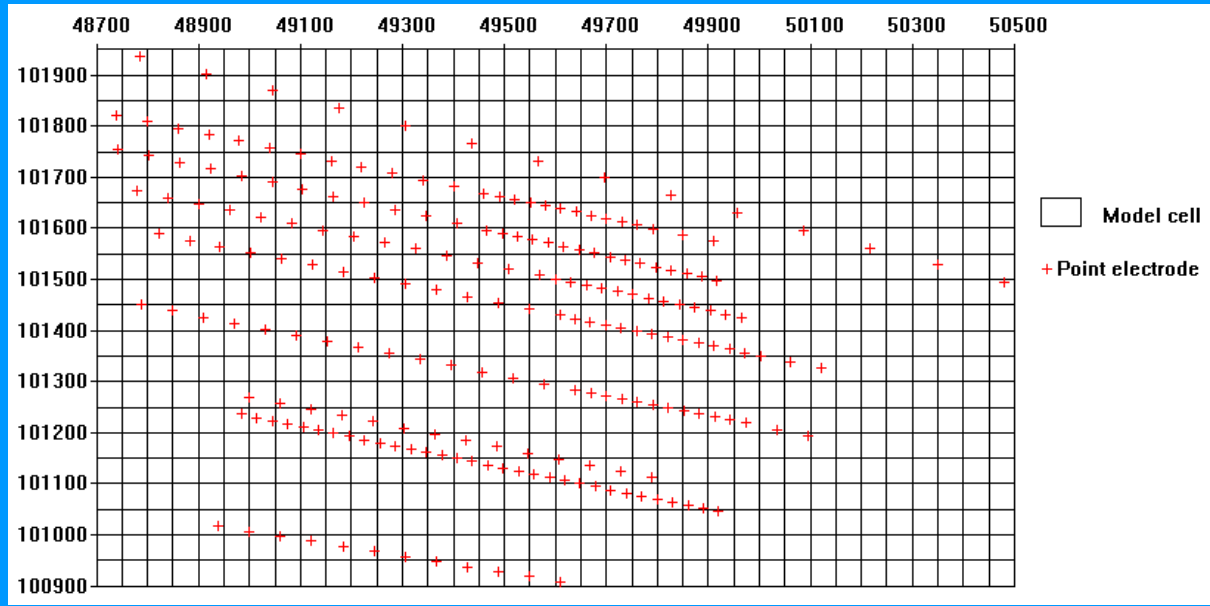

Methods to handle arbitrary electrode positions

There are two alternatives to model the effect of an electrode at an arbitrary position with the finite-element method. The first is to calculate the potential at the electrode by interpolating the potentials at the four nearest nodes in the mesh. The second method moves the nearest node to the location of the electrode using a distorted mesh.

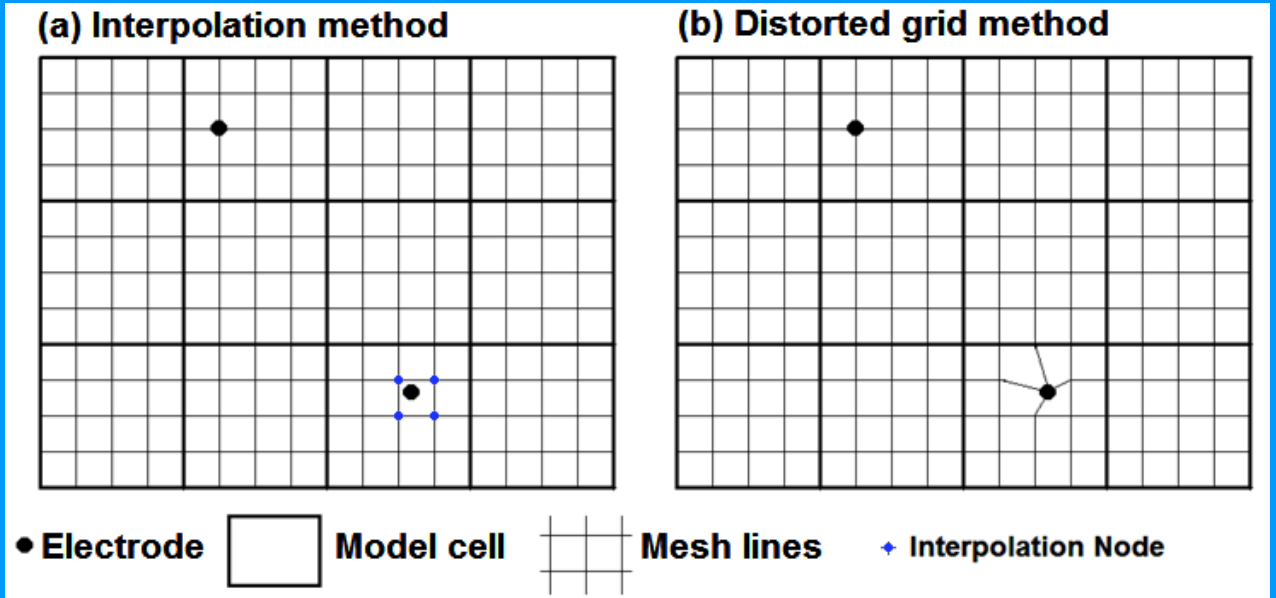

Burra copper deposit, SA

It is one of the oldest and largest copper mines in Australia, with active mining in the 1848-1877 and 1971-1981 periods. The main economic ores were malachite, azurite, cuprite, chrysocolla and native copper. Recently there has been some interest to renew mining in this area. The main lodes occur near the north-south Kingston Fault.

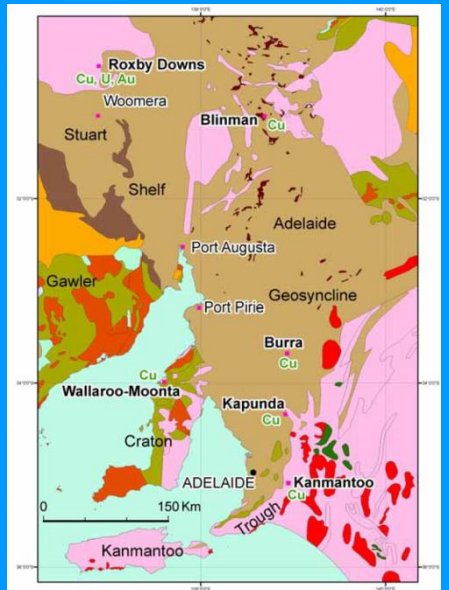

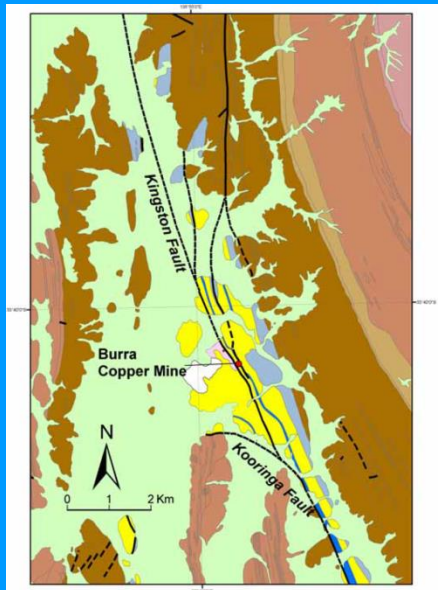

Burra copper deposit - surveys

In the 1960's, a number of I.P. surveys along 2-D lines were conducted. The lines from different survey phases had different spacings and directions.

A re-interpretation of the data was carried using modern 3-D inversion methods to glean more information from it.

Note the use of model cells of varying sizes, with smaller cells in areas of denser data coverage.

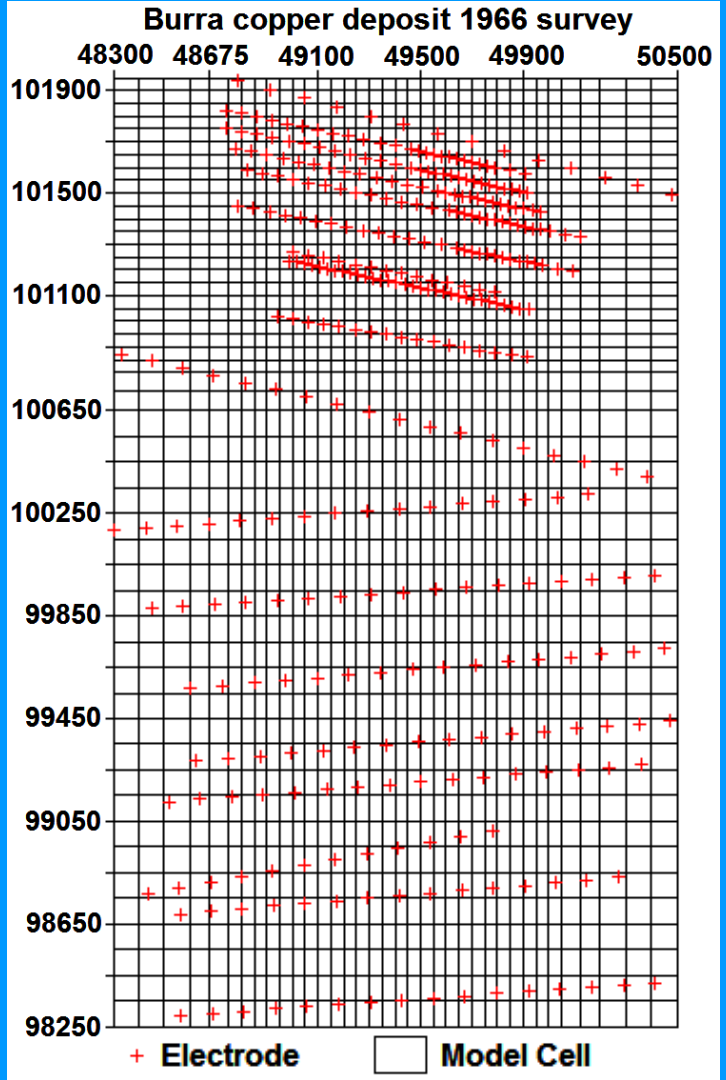

Burra copper deposit – resistivity model

The resistivity model is shown in the form of x-y (EW-NS) slices at different depths from the surface, starting from the left. The model show generally lower resistivity values along the approximately north-south Kingston fault.

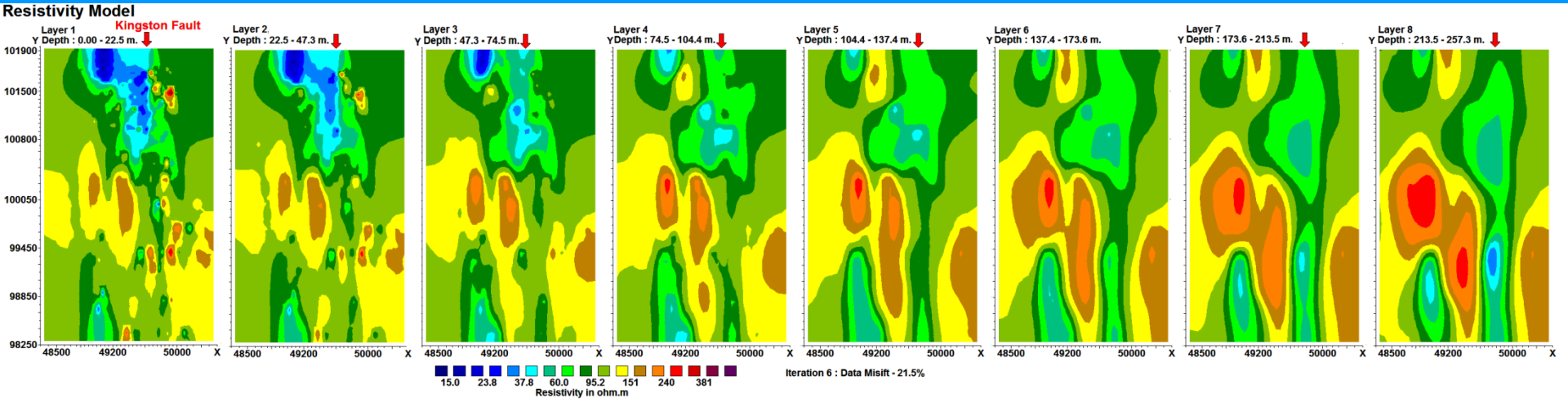

Burra copper deposit – I.P. model

A region with higher I.P. values in the northern third of the slices near the Kingston fault corresponds to the Eagle prospect. A drill hole by Phoenix Copper intersected sulphides. The I.P. anomalies towards the southern edge of the deeper layers is uncertain due to poor data coverage, although the easternmost anomaly lies in the Kingston Fault zone with sulphides found in a water bore.

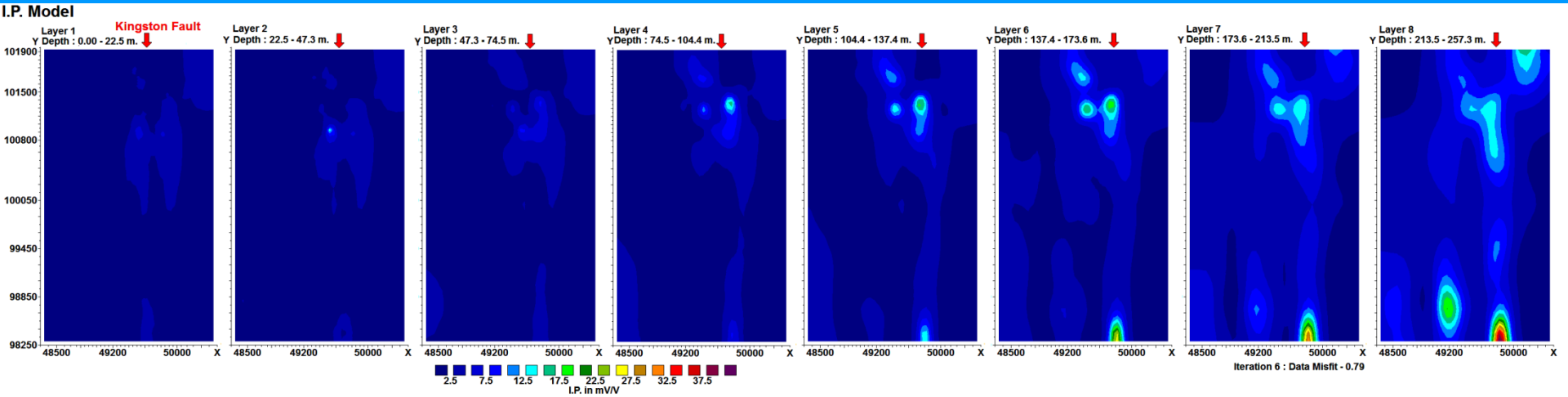

Burra copper deposit – model resolution index

Model resolution index = Model resolution x Cell volume correction factor x Number of model cells

A value of 1.0 indicates practically no resolution. Values of above 10-30 denotes regions with reasonable resolution. Layers with significant resolution extend to about 170 m. depth. Areas with high resolution values above 100 are clustered near the survey lines.

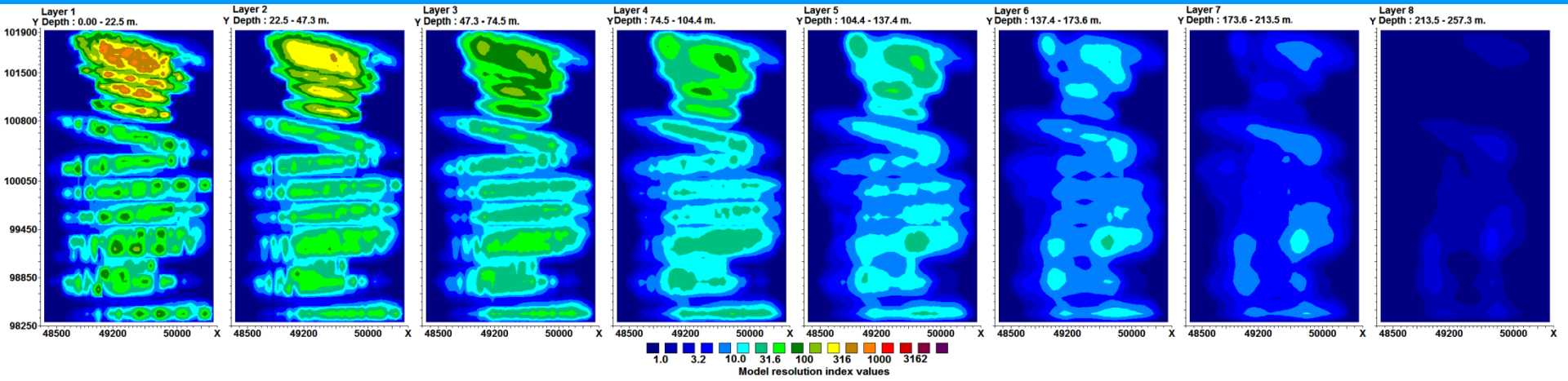

Burra copper deposit – 3-D plots

This shows 3-D plots of the resistivity and I.P. models. The Kingston fault is marked by a band of lower resistivity values.

The resistivity model generally reflects the general geology, while the I.P. model marks the locations of possible mineral deposits.

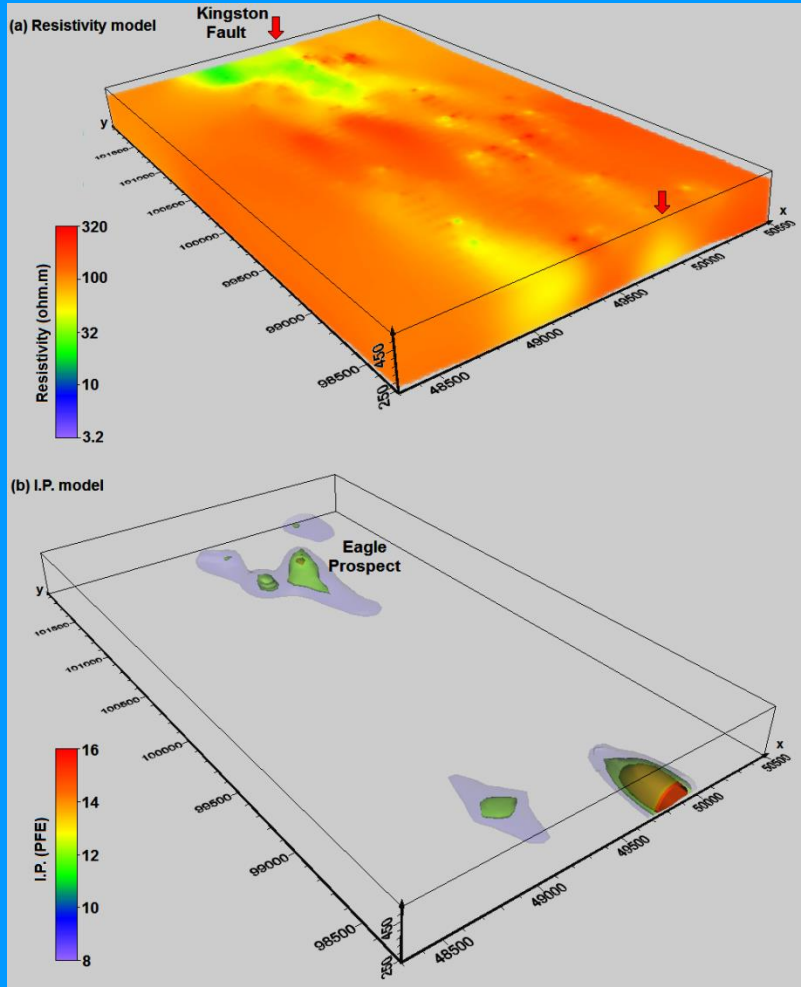

Smoothness constrained time-lapse method

The smoothness-constrained least-squares method equation is modified to include a time-lapse constraint.

$$\left[\mathbf{J}_i^T\mathbf{R}_d\mathbf{J}_i + \lambda_i\left(\mathbf{W}^T\mathbf{R}_m\mathbf{W} + \alpha\mathbf{M}^T\mathbf{R}_t\mathbf{M}\right)\right]\Delta\mathbf{r}_i = \mathbf{J}_i^T\mathbf{R}_d\mathbf{g}_i - \lambda_i\left(\mathbf{W}^T\mathbf{R}_m\mathbf{W} + \alpha_i\mathbf{M}^T\mathbf{R}_t\mathbf{M}\right)\mathbf{r}_{i-1}$$

M is the difference matrix applied across the time models. **R** is a weighting matrix. α is a damping factor that minimises the temporal changes to reduce artefacts.

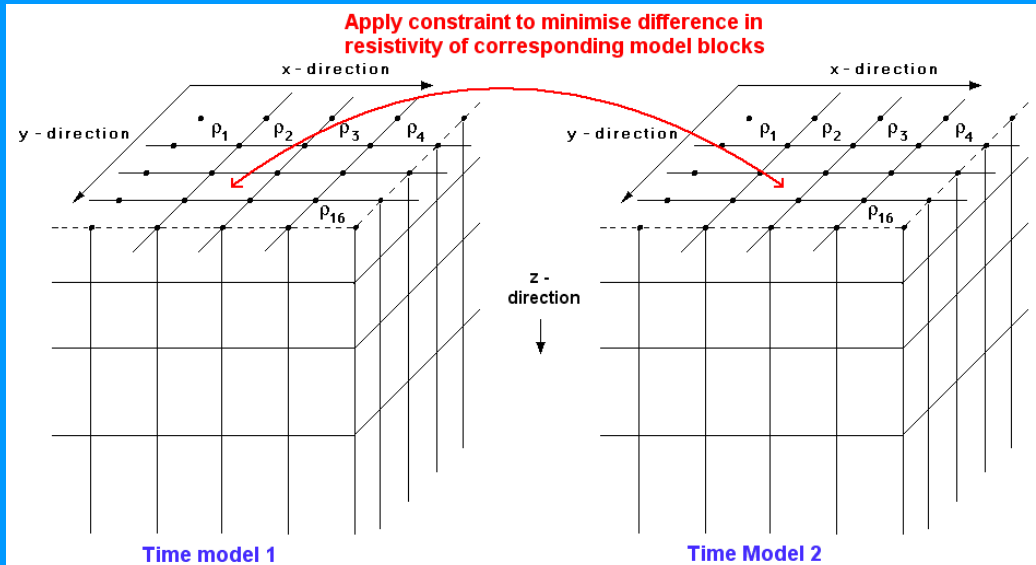

Cripple Creek, Colorado, USA

Sodium cyanide solution was injected into ore rock piles for secondary recovery of gold after surface leaching had ceased at the Cripple Creek and Victor Gold Mine. Resistivity measurements were made to monitor the flow of the solution to optimise gold recovery and ensuring safety of the side slopes.

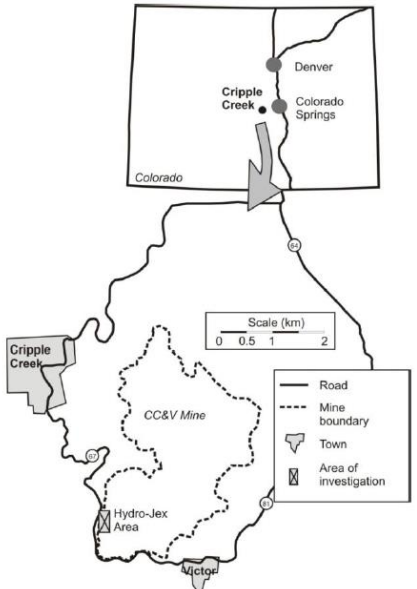

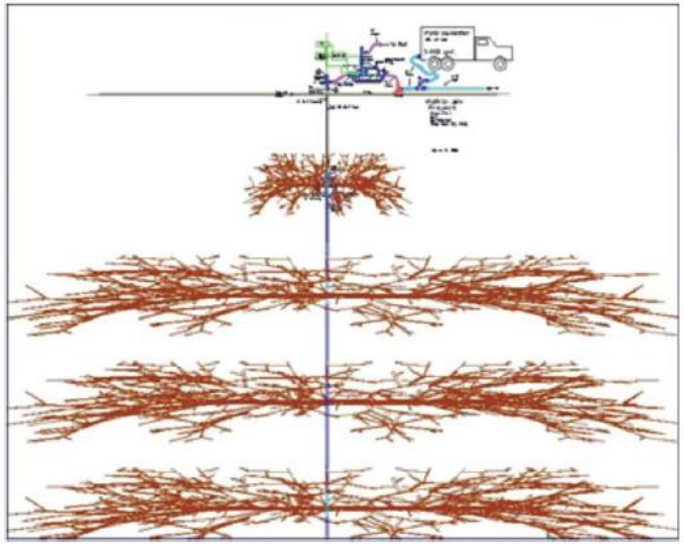

Cripple Creek, Colorado, USA – survey layout

Resistivity measurements were made using 48 surface electrodes placed along eight radials, 94 electrodes within six boreholes, and eight long electrodes using steel-cased injection wells.

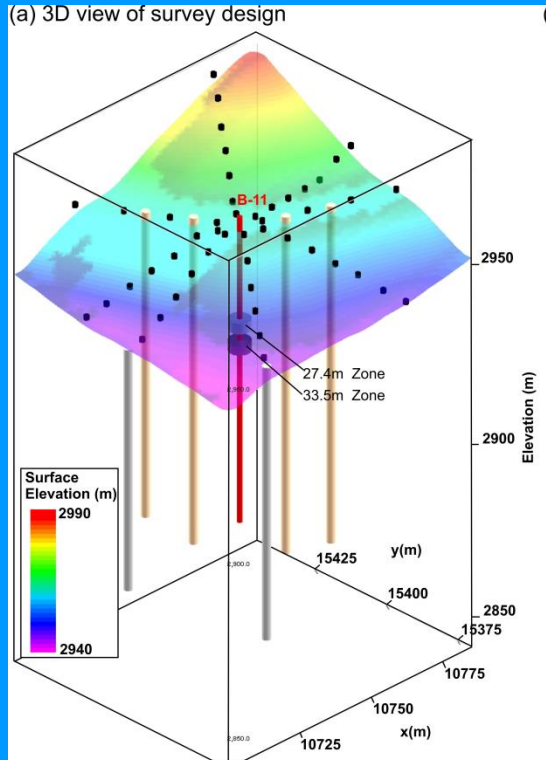

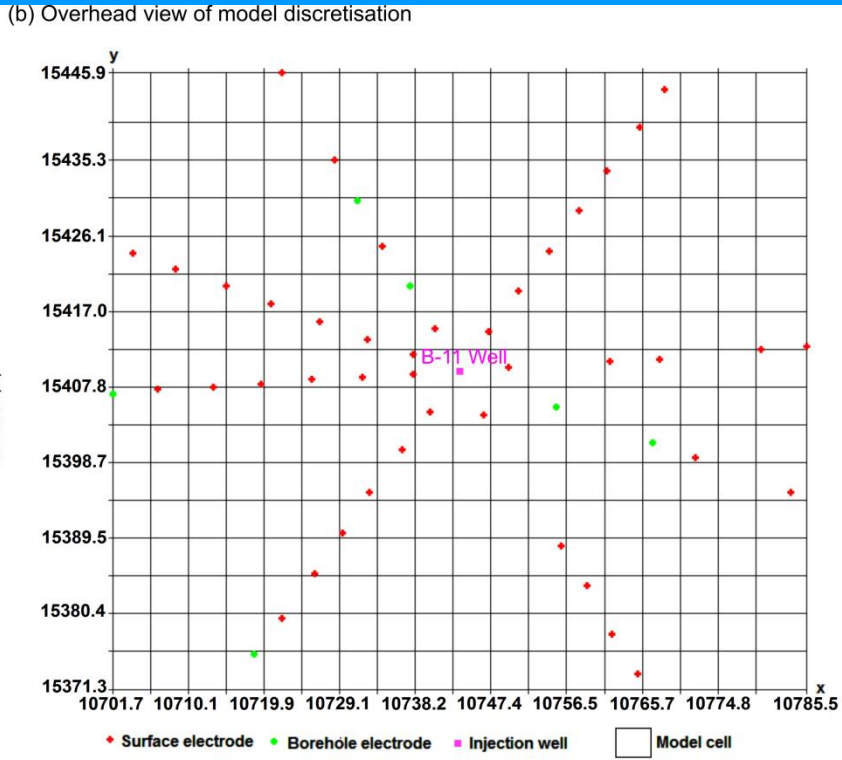

Cripple Creek, Colorado, USA – resistivity model

Shown below is an example of the resistivity sections in the form of x-z vertical slices. The low resistivity regions are due to the increased saturation from the previous seven days of injections.

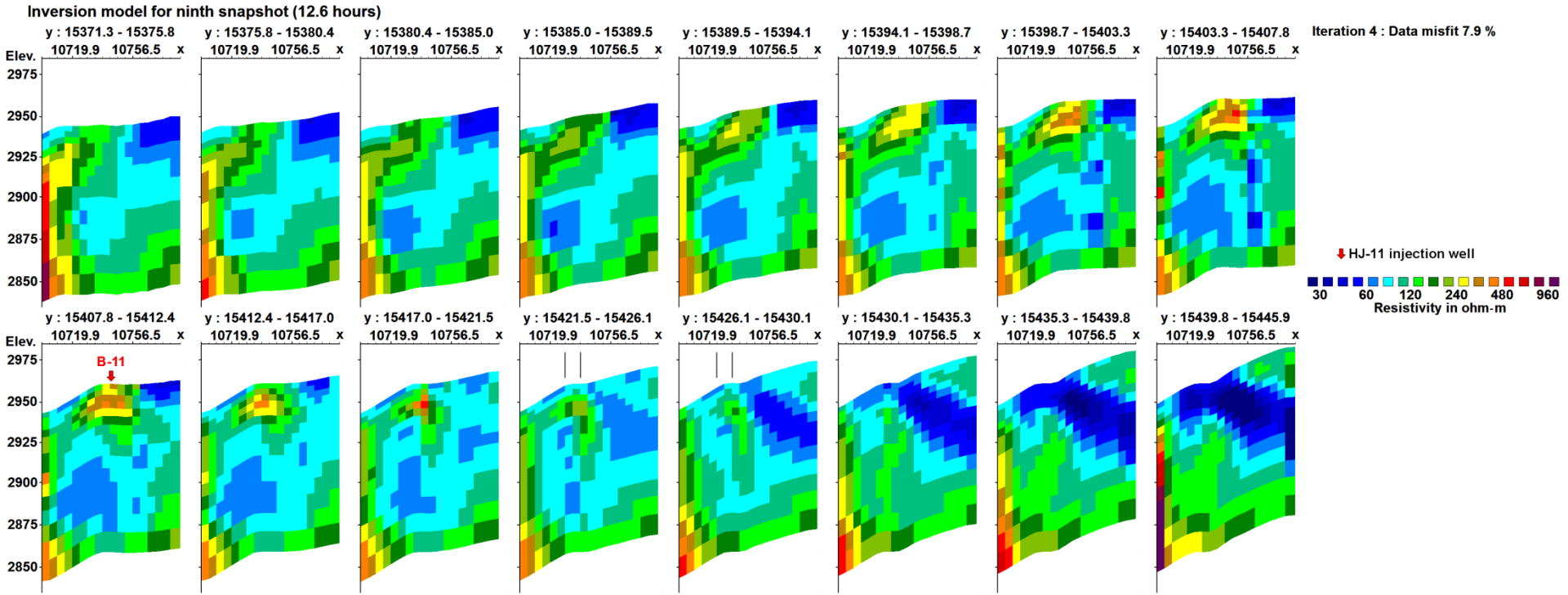

Cripple Creek, Colorado, USA – time-lapse models

As the ore heaps are highly inhomogeneous, the change in the resistivity is used to monitor the flow of the solution. Shown below are some results in the form of iso-surface contours for the -4% change in the resistivity at different times.

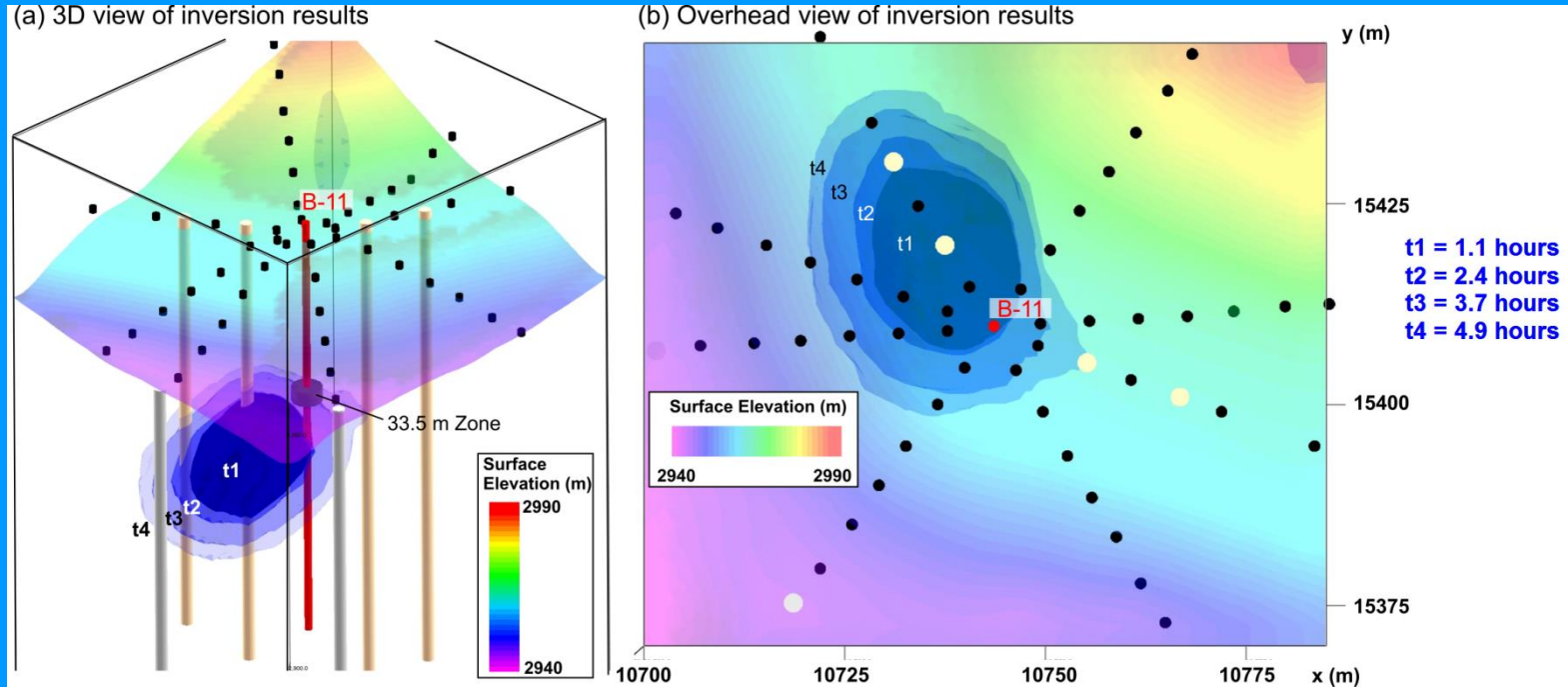

Cripple Creek, Colorado, USA – solution flow

The area with the largest change is located to the north of the well, probably due to differences in the subsurface permeability and structural nonuniformities within the heap created during end-dump construction.

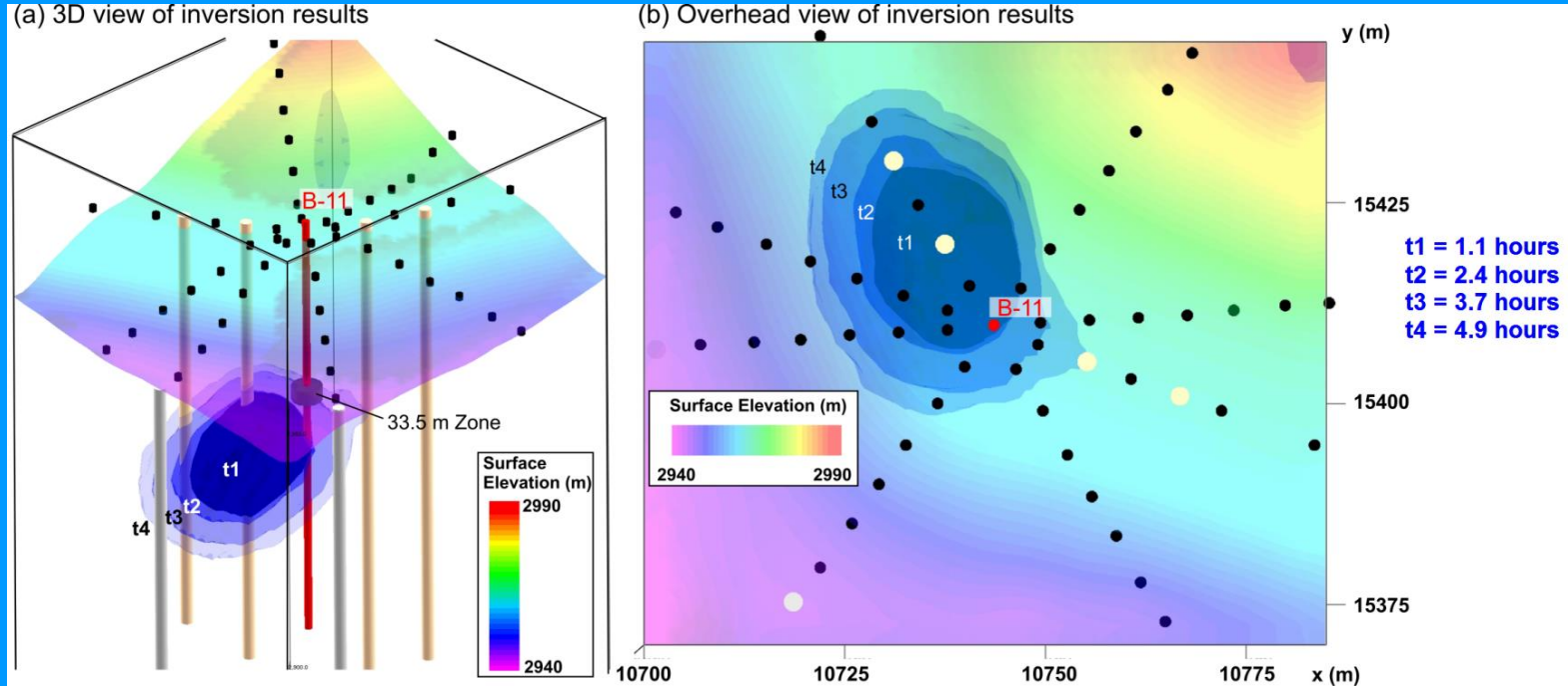

Tolukuma Au/Ag deposit, PNG

This is a low sulphidization epithermal Au/Ag deposit. Production is mainly from underground mines containing high grade, narrow veins. The veins are very narrow, but the region of mineralization that is picked up by the geophysical surveys is wider.

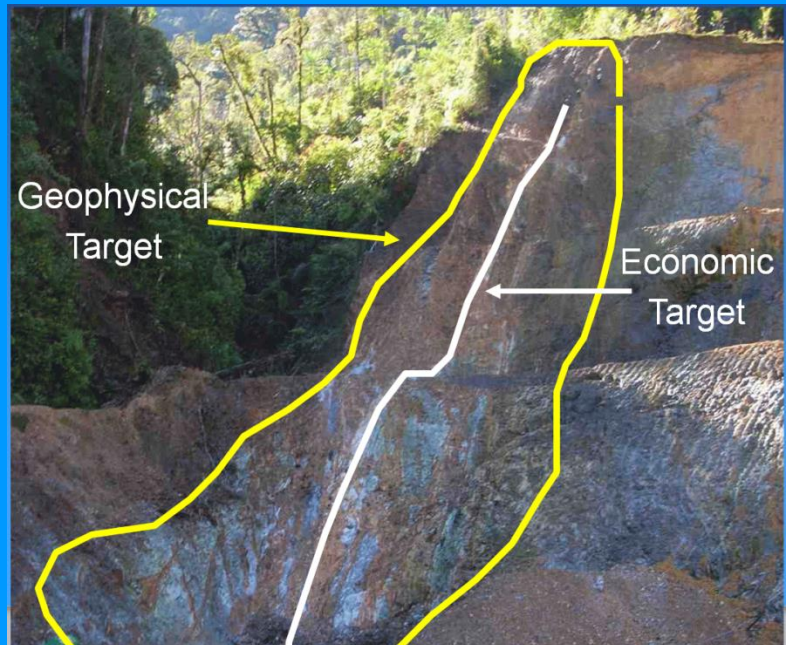

Tolukuma Au/Ag deposit - survey

The survey area is very rugged. An offset survey configuration is used with transmitter and receivers on separate lines.

First application in PNG of Search Exploration's 64 channel Receiver

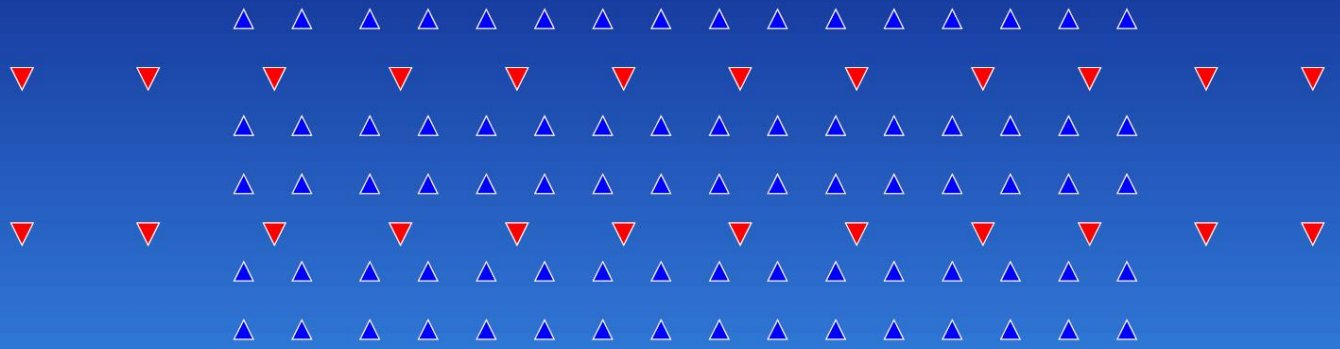

4 active receiver lines, 64 dipoles, each read by between 2 and 3 different transmitter lines -

Also first application of Search's multipole array in PNG -

Tolukuma Au/Ag deposit – model grid

The model grid uses cells with widths of 66 and 99 m. in the x and y directions.

Note the closer electrode spacings near the centre, and wider spacings at the sides.

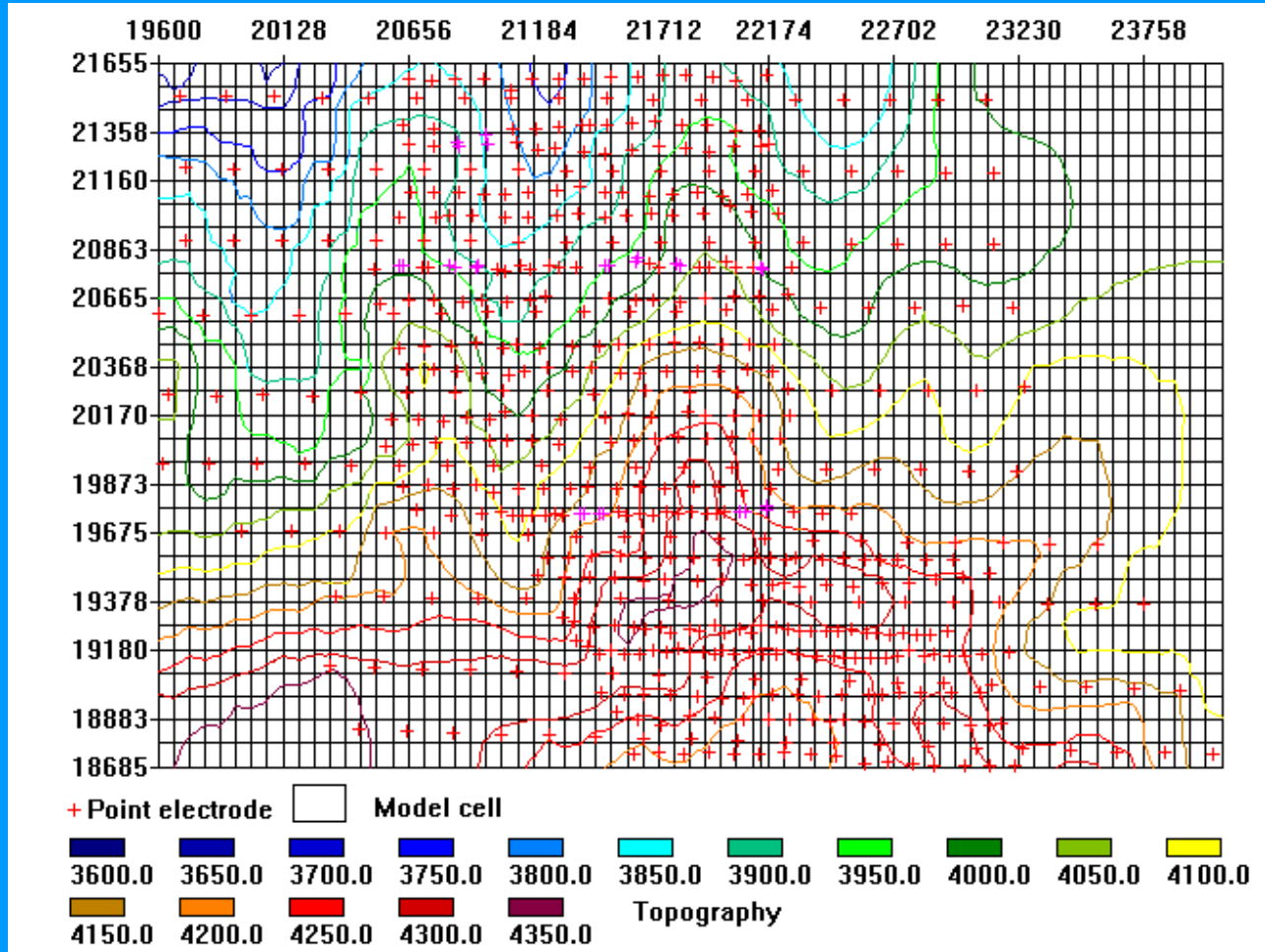

Tolukuma Au/Ag deposit – model grid resolution

A model with 12 layers was used with a maximum depth of 725 m. The plot shows the model resolution index for the layers, with the topmost layer at the top-left. There is a general decrease in the resolution with depth. The highest values in the top few layers are clustered near the survey lines. Low resistivity areas generally have higher resolution values.

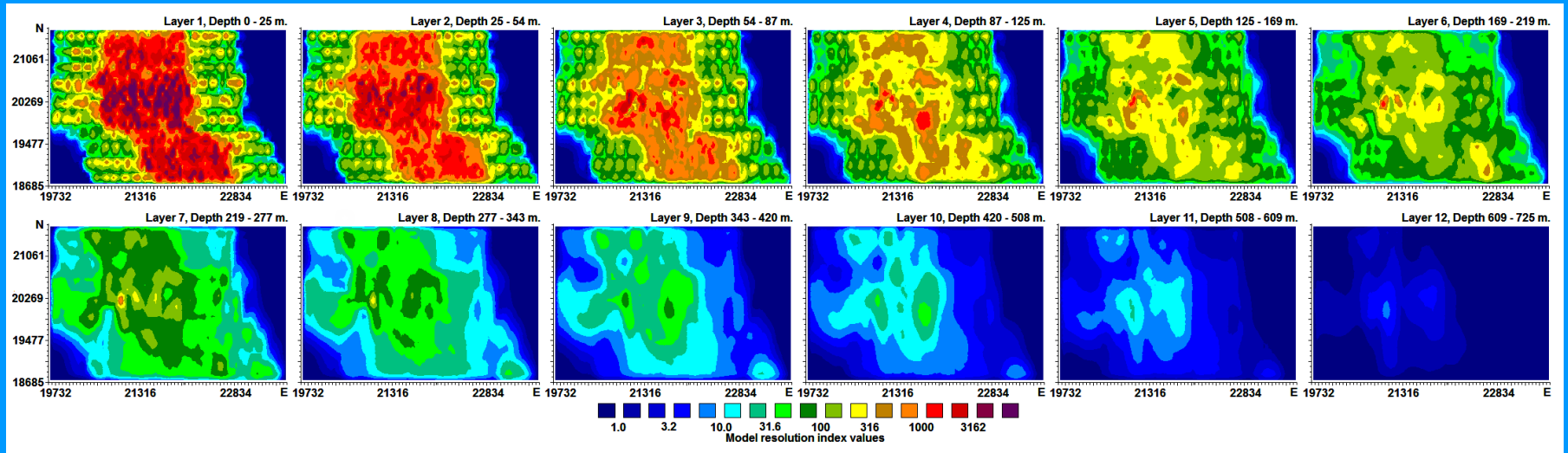

Tolukuma Au/Ag deposit – resistivity model

Below is a plot of the resistivity model for the layers. The model resolution was used to ‘fade out’ the regions with low resolution.

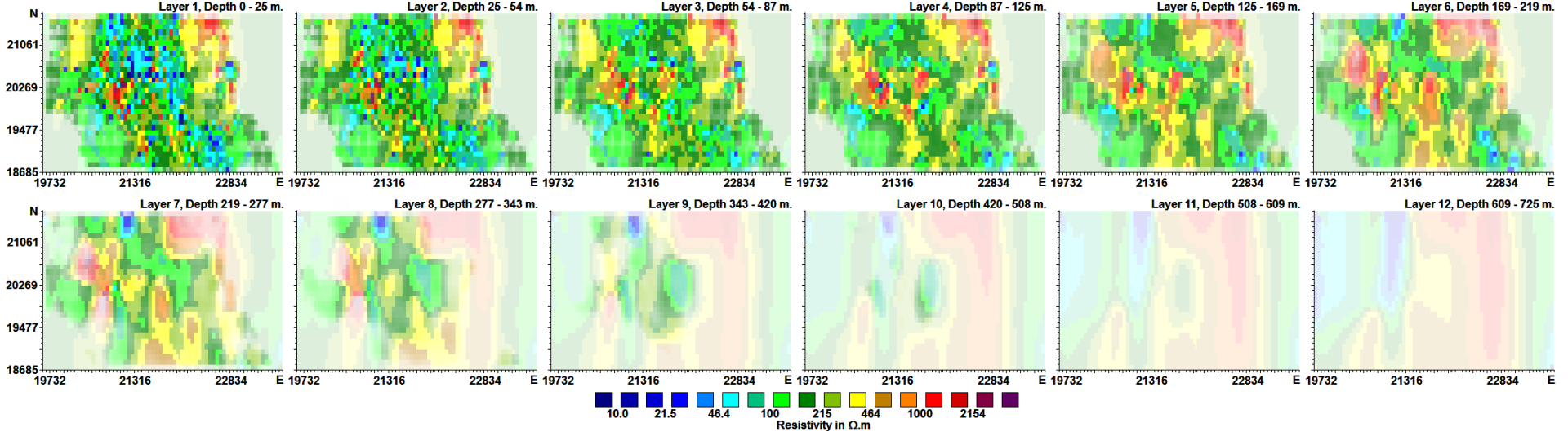

Tolukuma Au/Ag deposit – I.P. model

The I.P. model is more diagnostic, with a N-S band of higher values near a known mineralised vein. The very high I.P values in the bottom layers are uncertain due to very low resolution values.

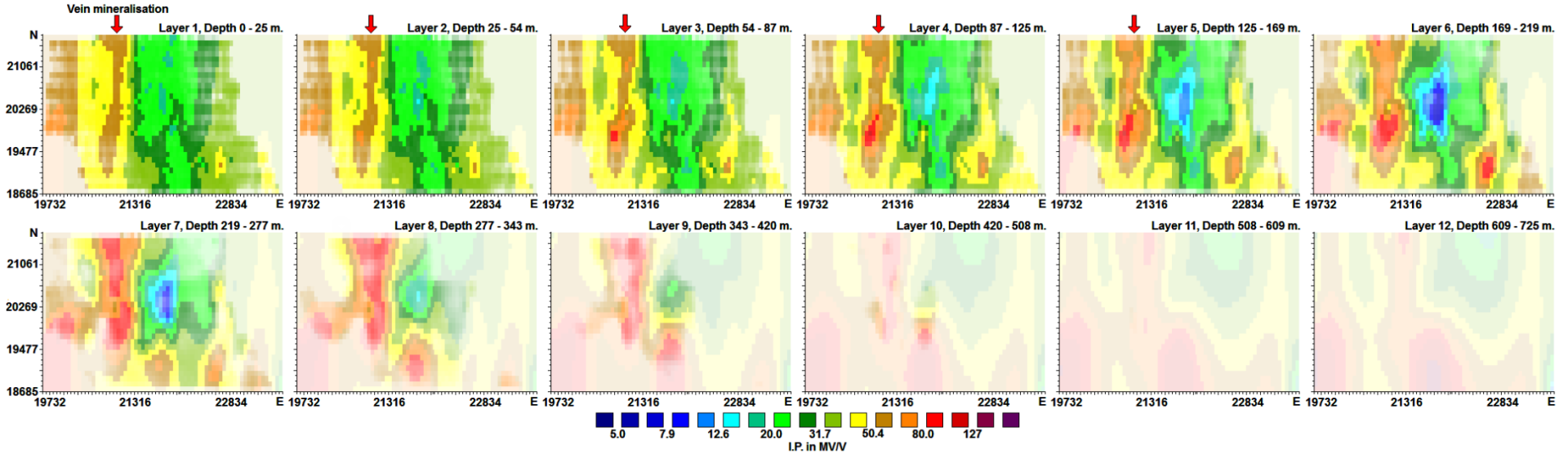

Tolukuma Au/Ag deposit – I.P. model with topography

This shows EW vertical sections of the I.P. model, with the northernmost section at the top-left. It shows more clearly the relationship between the band with higher I.P values with the surface location of the vein. Sulphides around a gold vein were encountered in a 500 m. deep borehole by Petromin.

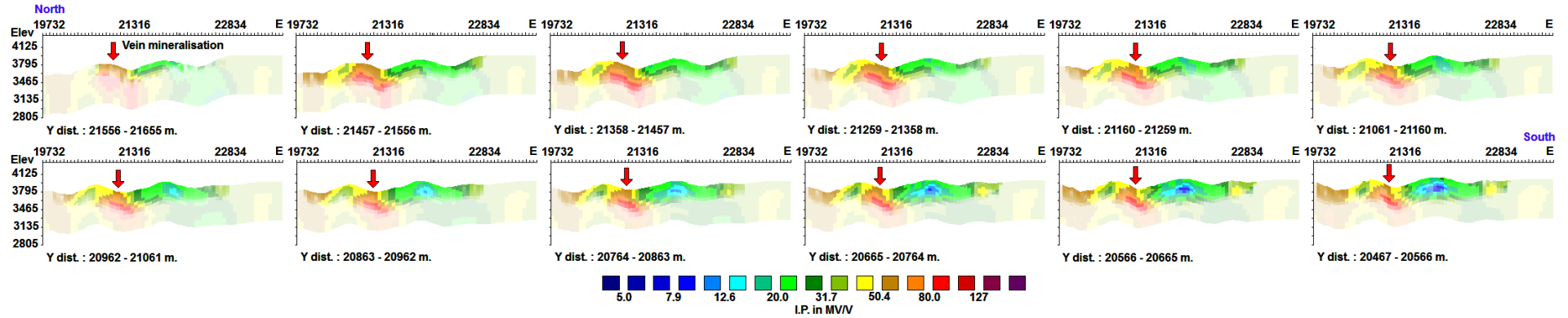

Conclusions

Modern interpretation of 3-D resistivity and I.P. surveys present several challenges that are met by the following methods.

The finite-element method can accurately model the topography.

A model discertisation that is independent of the electrode positions is used for a non-rectilinear arrangement of the electrodes.

The complex resistivity method can accurately calculate the I.P. effect, particularly for non-conventional arrays with large geometric factors.

The least-squares inversion method can be modified for time-lapse surveys.